The optical properties of Al_3Ni

1996 J. Phys.: Condens. Matter 8 2549

(http://iopscience.iop.org/0953-8984/8/15/006)

J. Phys.: Condens. Matter **8** (1996) 2549–2555. Printed in the UK

The optical properties of Al_3Ni

G Cubiotti†‡, A D Laine‡§, G Mondio‡§, E E Krasovskii‖,
O V Krasovska‖, Yu N Kucherenko‖, V N Antonov‖, Yu V Kudryavtsev‖
and V G Ivanchenko‖

† Dipartimento di Fisica dell'Università di Messina—Sezione di Fisica Teorica, PO Box 50, I-98166 S Agata di Messina, Italy
‡ INFM—Unità di Messina, Messina, Italy
§ Centro Siciliano per le Ricerche Atmosferiche e Fisica dell'Ambiente, Messina, Italy, and Dipartimento di Fisica della Materia, Geofisica e Fisica dell'Ambiente Salita Sperone 31, I-98166 S Agata, Messina, Italy
‖ Institute of Metal Physics, National Academy of Sciences of Ukraine, Vernadsky Street 36, 252142 Kiev, Ukraine

Received 4 October 1995, in final form 22 January 1996

Abstract. The optical properties of Al_3Ni have been deduced using spectrophotometry and ellipsometry and calculated within the extended linear augmented plane wave framework in the energy range 0–6 eV. Good agreement amongst all approaches is obtained up to about 2 eV, beyond which there is some divergence between theory and experiment where, for reasons discussed, the theory needs further refinement.

1. Introduction

As a consequence of their useful technological properties such as hardness and oxidation resistance, various compositions within the Al–Ni alloy system have been extensively examined, both theoretically and experimentally, and their electronic and optical properties have been the subject of several studies [1–7].

Most of this work has concentrated on the $AlNi_3$ [1–5] and AlNi [1] compositions because the former has interesting magnetic properties [2, 3] and also because they have relatively simple crystal structures (Cu_3Au and CsCl types, respectively). In comparison with the latter compositions, Al_3Ni, in addition to the fact that it is more difficult to handle experimentally due to its extreme brittleness, has a more complicated orthorhombic crystal structure with 16 atoms per unit cell which has only very recently been treated accurately [7]. Prior to this Al_3Ni had been modelled using the Cu_3Al crystal structure and its electronic properties have been calculated [1, 6]. A comparison of the density of states extracted from augmented spherical wave (ASW) [1] and linearized muffin tin orbitals (LMTO) [6] with experimental ultraviolet photoelectron spectroscopy (UPS) measurements [6] yielded only moderate agreement. Extended linear augmented plane wave (ELAPW) calculations performed with a real crystal structure [7] yielded much better agreement; the double-peaked structure of the DOS of the model calculations was replaced by a single smoother distribution as observed experimentally.

In this work, the ELAPW calculations are extended to calculate the optical properties of Al_3Ni up to the near-ultraviolet energy range and they are compared with experimental

0953-8984/96/152549+07$19.50

reflectivity and ellipsometry results in the same range. In section 2, the experimental details are given and in section 3 the theoretical framework is outlined. Both the theoretical and experimental results are described and discussed in section 4.

2. Experimental details

The Al_3Ni alloy sample, used for the spectrophotometric experiments, was prepared by melting the pure constituents in an argon arc furnace on a copper hearth. The composition was determined by weighing the constituents before melting and the compound after melting to establish the amount of any weight loss due to evaporation. The alloy was homogenized by repeatedly inverting and remelting the ingot while in the furnace. A flat slab was cut from the polycrystalline ingot and hand polished to a mirror finish prior to the measurements.

Reflectivity measurements were carried out at room temperature using a Perkin–Elmer infrared spectrophotometer and a Perkin–Elmer Lambda 2 UV–VIS–NIR spectrophotometer working in a double-beam mode with two near-normal-incidence reflectance accessories. Absolute reflectivities were obtained by normalizing the raw data to the reflectivity of a standard UV-coated aluminium mirror.

Standard ellipsometric measurements were carried out on a different sample prepared in a high-frequency vacuum furnace, annealed and polished after manufacture. This sample was not optically flat, which induced a noticeable degree of light scattering with a consequent loss of intensity in going towards UV energies.

3. *Ab initio* calculation of the optical properties

The imaginary part $\varepsilon_2(\omega)$ of the dielectric function has been calculated within the one-electron self-consistent-field approach [8]. The results presented have been averaged over the light polarizations. In the present calculation the self-consistent one-electron crystal potential was used, as obtained in a previous work [7]. To calculate the electron eigenenergies and wavefunctions the ELAPW method [9, 10] was used, but the number of energy-independent APWs was increased as compared to [7]. All the reciprocal lattice vectors $\boldsymbol{G}$, for which $|\boldsymbol{G}|S < 6.2$ were included, $S = 2.2$ a.u. being the radius of the smallest MT sphere. This yields 591 APWs and 54 localized functions are used to extend the basis set. The computational details are described in [7], where a reduced number (397) of APWs was used. The method of calculation of the momentum matrix elements in the ELAPW is similar to that in the usual LAPW [11, 12]. In constructing the spectrum an integration over the irreducible part of the Brillouin zone was made using the tetrahedron method [13] with a mesh of 196 $\boldsymbol{k}$-points (648 tetrahedra). The interband contribution to the real part of the dielectric function $\varepsilon_1(\omega)$ was obtained by Kramers–Kronig analysis. Seventy-five energy bands were calculated, of which bands from 37 to 40 are not completely filled. The finite number of bands yields underestimated values of $\varepsilon_2(\omega)$ for $\hbar\omega > 9$ eV, and the cut-off of the spectrum at 23 eV. Thus we estimate the Kramers–Kronig analysis to be valid up to 8 eV. In the energy range up to 9 eV the contribution to the f-sum rule amounts to 40%. The intraband contribution to the imaginary part of the dielectric function was neglected while the intraband contribution to the real part was calculated by the formula

$$\varepsilon_1^{int}(\omega) = 1 - \omega_p^2/\omega^2 \tag{1}$$

where ω_p is the plasma frequency. For a polycrystal

$$\omega_p^2 = \tfrac{1}{3}(\omega_{pxx}^2 + \omega_{pyy}^2 + \omega_{pzz}^2). \tag{2}$$

The diagonal element of the plasma frequency tensor for the electric field directed along the nth axis is determined by the integral over the Fermi surface

$$\omega_{pnn}^2 = \left(\frac{e}{\pi\hbar}\right)\sum_{\lambda} \mathrm{d}^2k \frac{V_n^2(k,\lambda)}{|V(k,\lambda)|} \tag{3}$$

with

$$V(k,\lambda) = \mathrm{d}E_\lambda(k)/\mathrm{d}k \tag{4}$$

where k is the band number and the summation is carried out over the sheets of the Fermi surface.

For orthorhombic Al_3Ni the results are $\hbar\omega_{pxx} = 5.02$ eV, $\hbar\omega_{pyy} = 5.15$ eV and $\hbar\omega_{pzz} = 3.66$ eV. The anisotropy of the optical properties has proved to be rather weak.

The optical conductivity spectrum has been calculated as

$$\sigma(\omega) = (\omega/4\pi)\varepsilon_2(\omega). \tag{5}$$

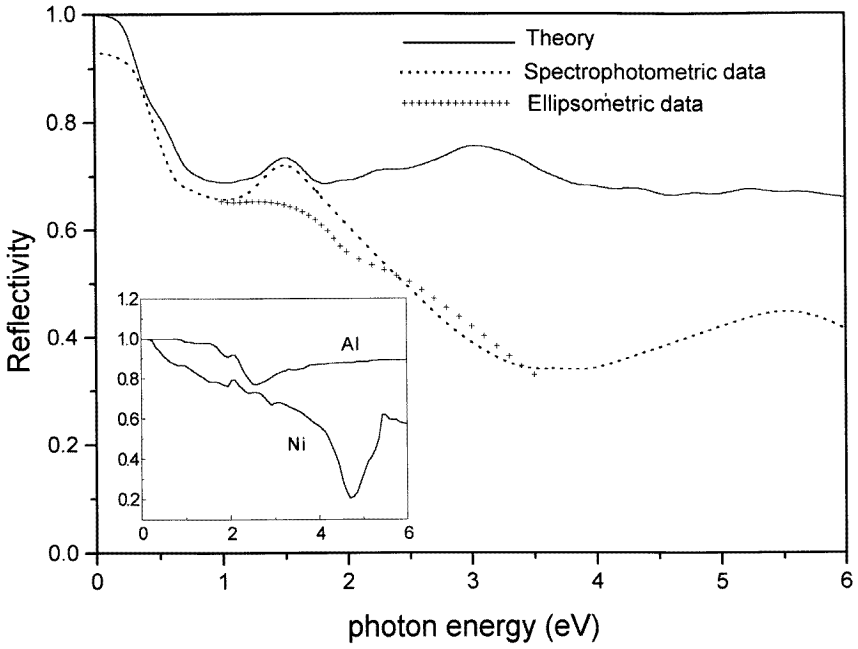

Figure 1. Experimental and theoretical data on the reflectivity of Al_3Ni are plotted as functions of the photon energy. Ellipsometric data run from 1.0 to 3.5 eV. The inset refers to theoretical results for pure constituents.

4. Results and discussion

Experimental reflectivity curves are shown in figure 1. The spectrophotometric data exhibit a decrease in reflectivity from 0.93 at very low energy to 0.65 at 1.0 eV followed by a peak at 1.5 eV, a steady fall to 0.35 at 3.5 eV and a broad peak with a maximum of 0.45 centred at 5.5 eV. The ellipsometric data coincide with the spectrophotometric data at 1.0 eV; there is a broad shoulder centred at 1.5 eV followed by a further shoulder at about

2.2 eV and a decrease in the reflection coefficient to 0.32 at 3.5 eV. General agreement with spectrophotometry is found in the region common to the two spectra. During the ellipsometric measurements the light intensity was weak after 3 eV and the data are expected to be least reliable in this region. Due to the above-mentioned limits and to the fact that the Kramers–Kronig procedure requires the experimental spectrum to be measured on a range as large as possible, only the spectrophotometric data have been considered to obtain dielectric constants and the optical conductivity.

The calculated reflectivity is also shown in figure 1 and, starting from values close to unity, falls to 0.70 at 1 eV and has a narrow peak at 1.5 eV and a broad peak centred at 3 eV. Beyond 1 eV there is little change in the magnitude of the reflectivity, which varies between 0.66 and 0.76. For comparison, the calculated reflectivity of pure constituents is also reported in the inset.

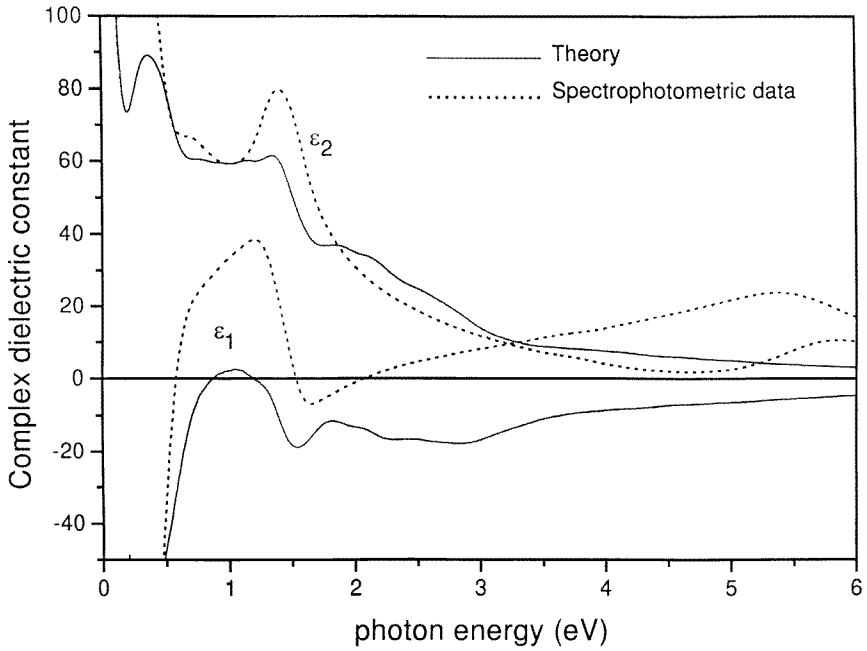

Figure 2. The comparison between theory and experiment for the functions ε_1 and ε_2, for different photon energies.

Complex dielectric constants, both experimental and theoretical, are shown in figure 2, as obtained from a rapidly converging Kramers–Kronig transform of the reflectivity data. A rapidly converging procedure is needed when the experimental range is not very wide and when the use of low- and high-energy tails is undesirable. Once the value of the phase ϕ_0 at a certain energy E_0 is known, the spectrum (E) is obtained by means of an expansion around E_0:

$$\phi(E) = \frac{E}{E_0}\phi_0 + \frac{E(E_0^2 - E^2)}{\pi} P \int_0^\infty \frac{\ln R(x)\,\mathrm{d}x}{(x^2 - E_0^2)(x^2 - E^2)} \tag{6}$$

where P indicates the Cauchy principal part of the integral. Taking for ϕ_0 the value deduced by ellipsometric measurements at 1.5 eV, the values of the real part and of the coefficient

of the imaginary part of the refractive index are deduced as

$$n(E) = [1 - R(E)]/(R(E) - 2\sqrt{R(E)}\cos\phi(E) + 1) \tag{7}$$

$$k(E) = 2\sqrt{R(E)}\sin\phi(E)/(R(E) - 2\sqrt{R(E)}\cos\phi(E) + 1) \tag{8}$$

and those of the dielectric constant as

$$\begin{aligned} \varepsilon_1(E) &= n(E)^2 - k(E)^2 \\ \varepsilon_2(E) &= 2n(E)k(E). \end{aligned} \tag{9}$$

The experimental ε_2 curve starts from high positive values, falls to 60 at 0.6 eV and is followed by peaks at 0.7 eV and 1.4 eV with a long tail to higher energies. The ε_1 curve starts at high negative values, is zero at 0.5 eV, rises to a maximum of about 40 at 1.3 eV after shoulders at 0.7 eV and 1.0 eV, has a minimum of about -10 at 1.6 eV and rises steadily to 25 at 5.3 eV followed by a gradual decline.

The theoretical data are qualitatively similar to the experimental data; the first peak in the ε_2 curve is displaced to lower energy and the second peak is much less intense. There is also more structure in the high-energy tail. The ε_1 data exhibit a lower, less structured maximum around 1 eV and there is also more structure in the tail which does not become positive. In figure 3 the experimental and theoretical optical conductivity results are reported.

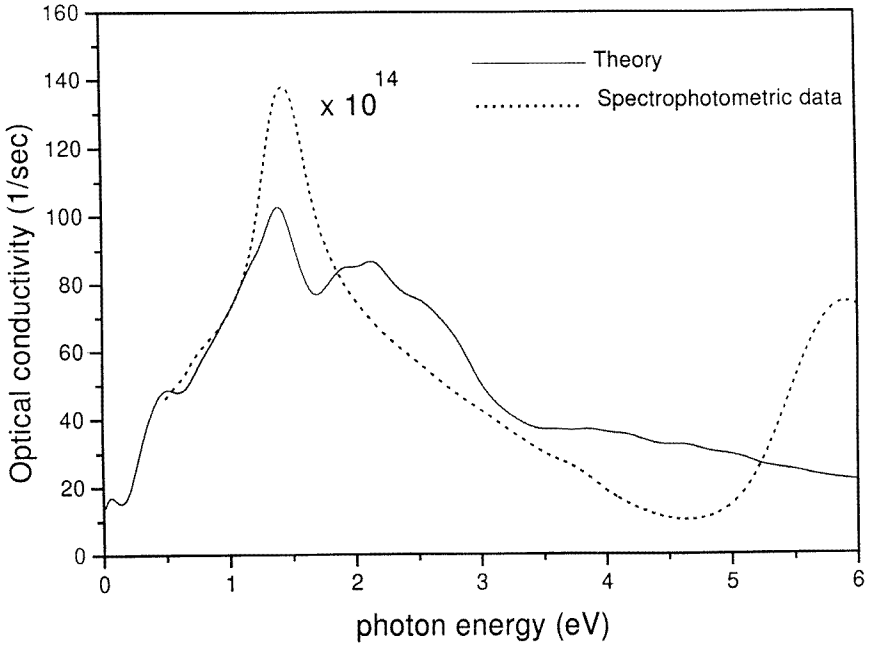

Figure 3. The comparison between theory and experiment for the optical conductivity as a function of the photon energy.

Much of the structure in the reflectivity spectrum is similar both qualitatively and quantitatively to that of elemental nickel including the features at 2.2 eV and 5.5 eV [14]. As is typical for metals, the reflectivity assumes, at low energy, values close to unity and the corresponding values of ε_1 and ε_2 diverge to very high negative and positive values as a consequence of free carrier absorption.

The structure at 1.5 eV in all the reflectivity data, the associated features at 1.4 eV in the ε_2 curve and the corresponding dispersion-like region in the ε_1 curve are due to transitions between partially filled free-electron-like bands. At this energy in pure aluminium there is a small drop in reflectivity due to a weak interband transition [14]. The shoulder at 2.2 eV in the ellipsometric data arises from states at the top of the Ni d band, which are strongly hybridized with the free-electron-like states. A similar behaviour is seen in the loss function as deduced by reflection electron energy loss spectroscopy [15].

In the present case, the overall agreement between theory and experiment for the reflectivity and dielectric constant is good to about 2 eV. If the number of basis functions used in the calculations is increased, the agreement between the calculated and experimental reflectivities improves due to a better representation of the electronic fine structure in the low-energy range. The convergence with respect to the number of basis functions depends on a number of factors relating to the system under consideration, amongst which are the crystal symmetry and the number of atoms per unit cell. For a pure metal, which has high crystal symmetry and a low number of atoms per unit cell, convergence is rapid [9] whereas in the present case the crystal symmetry is low and there are 16 atoms per unit cell. Obtaining convergence over a wide energy range is prohibitive in terms of computer time. In [7] the density of states calculated by the same ELAPW method is in good agreement with the experimental UPS specrum across the band. A comparison of the optical results with the theoretical data is, however, a much more stringent test of the calculation method than a UPS/DOS comparison. This is due to the superior resolution of the optical technique which probes the joint density of states which is more complex than the convolution of initial and final states probed by UPS.

Whereas the UPS/DOS comparison [7] is only a test for the energy position of the Ni d states in the valence band and for the width of this d subband, the optical functions reflect the fine structure of the energy distribution of the electron states in the valence band and in the energy region above the Fermi level. The calculated results for the reflectivity (figure 1) show a very good quantitative agreement with the experiment up to about 2 eV; at higher energies the theoretical values exceed the experimental ones. This disagreement takes place for all calculated reflectivity functions if the optical properties are described in terms of the transitions between one-electron states in the energy bands. More correct is a quasiparticle description of electron excitations with the finite lifetime (for the considered energy region the quasiparticle lifetime decreases with a proportional increase of the energy above the Fermi level). Taking into account the quasiparticle effects improves the agreement of the calculated results with experiment; however the calculations become more complicated, and the theoretical model should include some *ab initio* parameters.

In conclusion, a variety of techniques have been used to study the optical properties of the intermetallic compounds Al_3Ni. Its reflectivity has been measured and the complex dielectric constant and optical conductivity extracted. There is good qualitative agreement between experiment and the results of ELAPW calculations up to 6 eV photon energy and very good quantitative agreement up to about 2 eV. Due to the low crystal symmetry of the compound and the high number of atoms per unit cell, the calculations are very time consuming in the higher energy range so that agreement between theory and experiment is good, but not quite as good as for the density of states obtained within the same theoretical framework when compared to the experimental UPS spectrum.

Acknowledgment

One of the authors (ADL) would like to acknowledge the financial support of the Human Capital and Mobility Programme of the European Community under contract number ERBCHRXCT940563.

References

[1] Hackenbracht D and Kubler J 1980 *J. Phys. F: Met. Phys.* **10** 427
[2] Buiting J J M, Kubler J and Mueller F M 1983 *J. Phys. F: Met. Phys.* **13** L179
[3] Min B I, Freeman A J and Jansen H F J 1988 *Phys. Rev.* B **37** 6757
[4] Khan M A, Kashyap Arti, Solaki A K, Nautiyal T and Auluck S 1993 *Phys. Rev.* B **48** 16 974
[5] van der Heide P A M, Buiting J J M, ten Dan L M, Schreurs L W M, de Groot R A and de Vroomen A R 1985 *J. Phys. F: Met. Phys.* **15** 1195
[6] Andrews P T, Millar S C, Cubiotti G, Kucherenko Yu N, Yaresko A N and Antonov V N 1993 *J. Phys.: Condens. Matter* **5** 1935
[7] Cubiotti G, Krasowskii E E, Slobodyan O V, Kucherenko Yu N and Antonov V N 1995 *J. Phys.: Condens. Matter* **7** 4865
[8] Ehrenreich H and Cohen M A 1959 *Phys. Rev.* **115** 786
[9] Krasovskii E E, Yaresko A N and Antonov V N 1994 *J. Electron. Spectrosc. Relat. Phenom.* **68** 157
[10] Krasovskii E E and Schattke W 1995 *Solid State Commun.* **93** 775
[11] Andersen O K 1975 *Phys. Rev.* B **12** 3060
[12] Krasovskii E E, Antonov V N and Nemoshkalenko V V 1990 *Phys. Met.* **8** 882
[13] Lehmann G and Taut M 1972 *Phys. Status Solidi* b **54** 469
[14] Weaver J H, Krafka C, Lynch D W and Koch E E 1981 *Optical Properties of Metals. Physics Data (Fachinformationszentrum Karlsruhe)* vol 18 and references therein
[15] Laine A D, Mezzasalma A, Mondio G, Cubiotti G and Kucherenko Yu N to be published